Structural origin for the change of the order of ferroelectric phase transition in triglycine sulfate/selenate systems

2009 J. Phys.: Condens. Matter 21 335901

(http://iopscience.iop.org/0953-8984/21/33/335901)

J. Phys.: Condens. Matter **21** (2009) 335901 (8pp) doi:10.1088/0953-8984/21/33/335901

Structural origin for the change of the order of ferroelectric phase transition in triglycine sulfate/selenate systems

Rajul Ranjan Choudhury and R Chitra

Solid State Physics Division, Bhabha Atomic Research Center, Trombay, Mumbai 400085, India

Received 12 August 2008, in final form 7 July 2009
Published 27 July 2009
Online at stacks.iop.org/JPhysCM/21/335901

Abstract

Crystal structures of triglycine selenate (TGSe) and triglycine sulfate (TGS) obtained from single crystal neutron diffraction are compared. The double well single cell local potential experienced by the non-planar amino group of one of the three glycine ions (GI) of these two isostructural crystals is obtained using their crystal structure. It is suggested that the change in the nature of the ferroelectric phase transition as one goes from TGS to TGSe is due to the increase in the zero point energy resulting due to the change in the shape and height of the double well local potential of these crystals. Substitution of a selenate ion (SeO_4^{2-}) in TGSe by a sulfate ion (SO_4^{2-}) is considered as a source of an effective chemical pressure that can be utilized to tune the ferroelectric phase boundary in these crystals. The influence of alanine substitution on the ferroelectric phase transition in these crystals is investigated using differential scanning calorimetry.

1. Introduction

Proper ferroelectric phase transitions are the subclass of structural phase transitions where a phase change is heralded by the change in the point group symmetry of the crystals. This change results in the appearance of at least one non-zero component of spontaneous polarization (which is taken as the order parameter) in the ferroic phase [1]. Since the transition in proper ferroelectrics is mediated by the long-range cooperative interactions of dipolar origin, Landau's theory for phase transition is used successfully to study these transitions [1, 2]. It has been known for some time that a small change in the crystal structure from varying control parameters, such as the pressure or chemical composition, can lead to a significant change in the critical point phenomenon [1]. Landau's theory has been successfully modified [3] to incorporate the effects of such changes. Since Landau's theory is essentially a mean field theory which deals phenomenologically with macroscopic parameters relevant to a phase transition, correlating it to factors at the microscopic level, such as the unit cell structure, is not always straightforward. One needs models such as Onodera's model for ferroelectrics [4–7], or the Ising model for ferromagnets [1, 8, 9], to accomplish this task. These models have been successfully used [10, 11] to correlate the macroscopic properties and crystal structure at the unit cell level. In this communication we have tried to find a microscopic explanation for the observed differences in the critical point phenomenon in crystals belonging to a well-studied family of hydrogen bonded ferroelectrics, namely the triglycine sulfate family. The triglycine sulfate family includes crystals such as triglycine sulfate (TGS), triglycine selenate (TGSe), triglycine flouberyllate (TGFBe), mixed crystals such as TGS_xTGSe_{1-x} etc, doped crystals such as L-alanine doped TGS (LATGS) etc and deuterated crystals of parent compounds.

The ferroelectric phase transition in TGS, which is the most important member of this family of crystals, has been investigated extensively [1, 2, 12–17], as it is one of the model examples of a continuous second order phase transition [2]. But it is interesting to note that phase transition in TGSe [18], which is known to be structurally isomorphous to TGS [13], is not as clearly understood as that of TGS. The tricritical nature of the ferroelectric phase transition in TGSe has led to a resurgent interest in phase transition studies on this class of hydrogen bonded ferroelectric crystals [18–22].

Continuing our attempt to investigate the influence of structural changes on the phase transition properties of the TGS family [10, 11, 23, 24], single crystal neutron diffraction studies on crystals belonging to this family are undertaken. Differences between the structural parameters of TGS and

Table 1. Crystallographic and data collection details of TGSe single crystal neutron diffraction experiments.

Chemical formula	$H_{17}C_6N_3O_{10}Se_1$	Diffractometer	Four circle
M_r	461.15	Data collection method	θ–2θ scan
Space group	Monoclinic $P2_1/m$	No. of measured, independent and observed reflections	1745, 1745, 1745
Temperature (K)	300	Criterion for observed reflections	$I > 2\sigma(I)$
a, b, c (Å), α, β, γ (deg)	5.853, 12.813, 9.235, 90, 105.6, 90.00	R_{int}, $R1(1073)Fo > 4\sigma(Fo)$, wR2	0.00, 0.088, 0.308
V (Å^3)	666.8	$\theta_{\max}$ (deg)	41.81
Z	2	No. and frequency of standard reflections	2 every 25 reflections
D_x (Mg m^{-3})	2.297 Mg m^{-3}	Intensity decay (%)	<3%
Radiation type	Neutron	GOOF	1.079

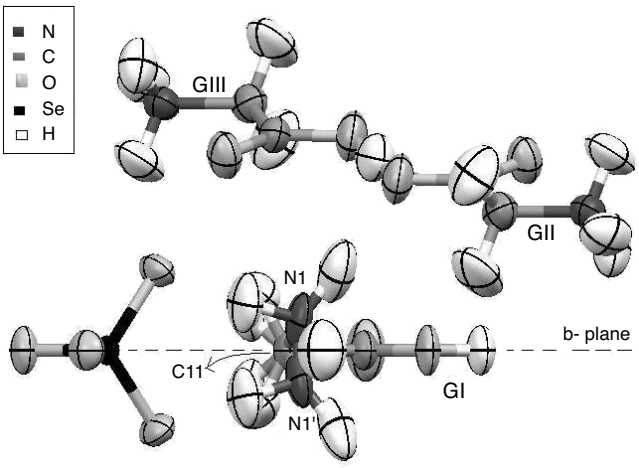

Figure 1. An asymmetric unit of the TGSe unit cell in the paraelectric phase.

TGSe, obtained from careful single crystal neutron diffraction investigations, are reported here. In order to correlate these fine structural changes at the unit cell level to the observed differences in the critical point phenomenon of these crystals we have defined a single cell static mean field Hamiltonian H_L for these crystals. The potential energy term of the Hamiltonian H_L is separated into a local (Vs) and cooperative contribution. The local potential energy term Vs is approximated as the double harmonic potential and the tunneling frequency for TGS and TGSe is estimated.

The effect of different levels of a dopant, such as L-alanine, on the phase transition properties of TGS and TGSe is investigated using differential scanning calorimetry. The results are analyzed from the viewpoint of the crystal structures obtained from the single crystal investigation.

2. Single crystal neutron diffraction investigation

Crystals of TGS and TGSe were grown by the method of slow evaporation from aqueous solutions of glycine and sulfuric acid, and glycine and selenic acid, respectively. Details of single crystal neutron diffraction data collected on TGS are published elsewhere [25]. Ambient temperature single crystal neutron diffraction investigations on TGSe were undertaken; this to the best of our knowledge is the first ever single crystal diffraction study of TGSe. A clear rectangular single crystal of TGSe was loaded on a goniometer, which was then mounted on a four-circle single crystal diffractometer with a BF_3 point detector located at the Dhruva reactor at Trombay. Crystallographic details and data collection details are given in table 1.

Table 2. A comparison between the unit cell parameters of TGS and TGSe.

	a (Å)	b (Å)	c (Å)	β (deg)	V (Å^3)
TGSe	5.8525(10)	12.8133(4)	9.2349(9)	105.6(1)	666.8(6)
TGS	5.7339(7)	12.6436(5)	9.1666(10)	105.5(1)	640.1(7)

The structure was solved using direct methods, as implemented in the structure solution software SHELXS [26]. The initial model obtained contained the coordinates of all the non-hydrogen atoms. This model was then subjected to a series of isotropic and anisotropic least squares refinement using the software SHELXL [26]. From the difference Fourier map all the hydrogen atoms were located and refined anisotropically (figure 1). The nuclear scattering lengths used are $b_N = 0.936 \times 10^{-12}$ cm, $b_C = 0.6646 \times 10^{-12}$ cm, $b_H = -0.3739 \times 10^{-12}$ cm, $b_{Se} = 0.7973 \times 10^{-12}$ cm and $b_O = 0.5803 \times 10^{-12}$ cm. All the reflections including negative F^2o are used for refinement. In the initial stages of refinement the weight (w) was taken to be $1/\sigma(F^2o)$, which was derived using counting statistics.

In order to compare the reported structure of TGS [25] to the structure of TGSe detailed here we have transformed the coordinates and unit cell parameters of TGS to a coordinate system identical to that of TGSe. Also the origin of the TGS coordinate system has been shifted to match that of the TGSe coordinate system. Tables 2 and 3 give a comparison between TGS and TGSe unit cells and structures, respectively.

The most important conclusion derived from the comparison between the unit cell parameters of TGSe and TGS is that substitution of a SO_4^{2-} ion (molecular volume 62.0 Å^3) by a larger SeO_4^{2-} ion (molecular volume 66.8 Å^3) results in a swelling of the unit cell, as is evident by the increase in the lengths of the unit cell vectors a, b and c, although there is no change in the shape of the unit cell since angles α, β, γ remain unchanged.

Table 3. A comparison between the atomic coordinates of TGS and TGSe. Standard deviations in the atomic coordinates are of the order of the third or fourth decimal place. ΔR_i is the distance between equivalent atoms (n) in the two unit cells from a common origin.

TGSe neutron structure at 300 K				TGS neutron structure at 300 K				
Atom	x/a	y/b	z/c	Atom	x/a	y/b	z/c	ΔR_i
Se	0.7254	0.7500	0.5005	S	0.7241	0.7447	0.5001	0.211
O1Se	1.0142	0.7500	0.5388	O1S	0.9908	0.7436	0.5345	0.315
O3Se	0.6409	0.7500	0.6560	O3S	0.6489	0.7470	0.6425	0.231
O2Se	0.6113	0.8536	0.4068	O2S	0.6258	0.8400	0.4123	0.318
O3Se	0.6113	0.6464	0.4068	O3S	0.6239	0.6501	0.4152	0.080
N2	0.7008	1.0701	1.3985	N2	0.6978	1.0662	1.3957	0.260
C4	0.8655	1.0294	1.1871	C4	0.8699	1.0267	1.1825	0.239
C3	0.6542	1.0700	1.2342	C3	0.6512	1.0646	1.2311	0.274
O21	1.0455	1.0033	1.2805	O21	1.0557	1.0011	1.2783	0.222
O22	0.8287	1.0277	1.0436	O22	0.8387	1.0271	1.0395	0.208
O31	0.9545	0.9967	0.7195	O31	0.9523	0.9976	0.7131	0.206
O32	1.1713	0.9723	0.9564	O32	1.1895	0.9758	0.9487	0.176
N3	1.2992	0.9299	0.6015	N3	1.2898	0.9228	0.5839	0.345
C5	1.1345	0.9706	0.8129	C5	1.1408	0.9707	0.8023	0.222
C6	1.3458	0.9300	0.7658	C6	1.3494	0.9263	0.7500	0.287
H1	1.0000	1.0000	1.0000	H1	1.0320	1.0021	0.9882	0.254
H6	0.4993	1.0233	1.1863	H6	0.5001	1.0156	1.1811	0.296
H2	0.8372	1.1192	1.4437	H2	0.8433	1.1177	1.4397	0.243
H3	0.5630	1.0994	1.4319	H3	0.5558	1.0996	1.4288	0.223
H7	0.6117	1.1487	1.1917	H7	0.6040	1.1450	1.1878	0.273
H4	0.7327	0.9954	1.4401	H4	0.7306	0.9929	1.4389	0.229
H7	1.3883	0.8513	0.8083	H7	1.3894	0.8480	0.7944	0.272
H2	1.1628	0.8808	0.5563	H2	1.1462	0.8732	0.5441	0.338
H3	1.4370	0.9006	0.5681	H3	1.4299	0.8933	0.5472	0.358
H6	1.5007	0.9767	0.8137	H6	1.5073	0.9743	0.7930	0.310
H4	1.2673	1.0046	0.5599	H4	1.2463	0.9963	0.5388	0.406
C1	1.1208	1.2500	0.9800	C1	1.1170	1.2563	0.9893	0.197
C2	0.9268	1.2500	0.8350	C2	0.9263	1.2509	0.8407	0.224
N1	0.7019	1.2095	0.8585	N1	0.6944	1.2095	0.8578	0.234
N1′	0.7019	1.2905	0.8585	N1′	0.6926	1.2854	0.8561	0.310
O11	1.0425	1.2500	1.0991	O11	1.0306	1.2525	1.1066	0.250
O12	1.3285	1.2500	0.9831	O12	1.3285	1.2620	0.9944	0.168
H11	0.7291	1.1473	0.9296	H11	0.7218	1.1428	0.9230	0.288
H10	0.5901	1.1883	0.7578	H10	0.5767	1.1915	0.7543	0.211
H9	0.6170	1.2500	0.9017	H9	0.6066	1.2610	0.9099	0.144
H8A	0.8972	1.3265	0.7839	H8a	0.8929	1.3289	0.7916	0.231
H8B	0.9794	1.2015	0.7585	H8b	0.9853	1.2009	0.7654	0.224
H5	1.1739	1.2500	1.1981	H5	1.1644	1.2523	1.2077	0.255
H11p	0.7291	1.3527	0.9296					
H8Ap	0.8972	1.1735	0.7839					
H10p	0.5901	1.3117	0.7578					
H8Bp	0.9794	1.2985	0.7585					

The isostructurality index [27], defined by the following equation, gives a measure of similarity between two structures:

$$I_i(n) = \{1 - (\Sigma \Delta R_i^2/n)^{1/2}\} \times 100\%. \quad (1)$$

Here ΔR_i is the distance between equivalent atoms (n) in the two unit cells from a common origin. The value of $I_i(38) = 70\%$ for TGS and TGSe crystals, indicating a high form of isostructurality between the two.

Since the primary effect of the substitution of SO_4^{2-} by SeO_4^{2-} is the increase in the unit cell volume with the shape remaining unchanged, this substitution can be equated to a net effective chemical pressure, which dilates the unit cell. This chemical pressure can be utilized to tune the ferroelectric phase boundary in this class of ferroelectric crystals by varying the extent of selenate substitution. The TGS/TGSe mixed system is similar to the alloy system of the prototype compound tetrathiafulvalene-*p*-chloranil (TTF)-(QCl4), formed by incorporating the selenium analogue of TTF, namely tetraselenafulvalene (TSF), into the system [28, 29]. As compared to TTF, TSF has a larger molecular volume but a minimized perturbation, such as the molecular shape, symmetry, and ionization energy; the same applies for SO_4^{2-} and SeO_4^{2-} ions as well.

In the subsequent sections we have tried to analyze the effect of these changes, at the microscopic unit cell level, on the phase transition in the TGS family. Recently Toshio *et al* explicitly [30] found the structure of negative as well as positive domains of TGS in the ferroelectric phase by performing x-ray diffraction under two electric fields of opposite polarities. They clearly showed that the main structural change on polarization reversal is the rotation of GI resulting in the change of the amino group position from one side of the *b*-plane to the other, and a flip-flop motion of

the hydrogen atom between glycine ions labeled GII and GIII. These two motions are correlated [10] and in all likelihood the former drives the latter. It is assumed that in the paraelectric phase GI, as well as the hydrogen connecting GII and GIII, continuously move back and forth between the two above stated sites [2] corresponding to the two opposite polarity domains. The structure of TGSe in the paraelectric phase reported here supports this assumption. The nitrogen atom N1 of GI is disordered about the *b*-plane, the elongated shape of its thermal ellipsoid (figure 1) suggests that the disorder is in all likelihood dynamic. The hydrogen atom between GII and GIII occupies a symmetric position between the two molecules; its thermal ellipsoid is also elongated along the line joining the two molecules, indicating dynamic disorder.

3. Local potential energy landscape for TGS/TGSe systems

In our previous communications [10, 11] we estimated the potential $Vs(\mathbf{r})$ experienced by the amino group of GI in TGS using the then available neutron structure of TGS, which was of a very limited resolution, whereas in order to find the potential energy landscape in TGSe we used the structure obtained from the Rietveld refinement of the x-ray powder diffraction data. We have now conducted careful single crystal structural investigations on TGS as well as TGSe, and in this section we have re-estimated the local potential energy landscape in TGS and TGSe using the precise structure obtained through careful neutron diffraction investigation.

In order to obtain $Vs(\mathbf{r})$ we calculated the energies of the hydrogen bonds made by the three hydrogen atoms of the $-NH_3^+$ group of GI [10] as it flips between its equivalent sites about the *b*-plane (figure 1). Hydrogen-bond energies are calculated using the semi-empirical potential function, namely the modified Lippincott and Schroeder function [31, 32] described below:

$$Vhb = D_0\{1 - \exp[-n(x - r_0)^2/2r]\} + CD_0'\{-\exp[-n'(d - r_0')^2/2Cd]\} - B/R^6 + A\exp\{-aR\}.$$

Values of potential parameters D_0, r_0, C, B, A, as reported by Ramanadham and Chidambaram [10, 33] are used for calculation. R denotes the donor and acceptor distance, d denotes the hydrogen atom and acceptor atom distance and x denotes the hydrogen atom and donor atom distance.

The intermediate positions of the $-NH_3^+$ groups are generated by assuming that the nitrogen atom of the group moves along the arc N1–N1′ of a circle with its center at C1 and radius equal to the C1–N1 bond length (figure 1). All the hydrogen positions used in the calculations are generated by assuming an ideal staggered geometry for the amino group with the average N–H distance taken as 1.014 Å. The observed deviation of the hydrogen atoms from the staggered geometry at the two minimum energy positions (N1 and N1′) is small (within ±11°) and hence it is expected that the above simplification will not lead to a major difference between the energies of the actual and calculated systems. The net potential energy (table 4) of the $-NH_3^+$ group is taken as the sum of the hydrogen-bond energies. The local potential energy ($Vs(\mathbf{r})$) landscape for the $-NH_3^+$ group is of the symmetric double minimum kind. Figure 2 gives a comparison between the local potential energy landscapes in TGS and TGSe. The main difference between the two is the reduction in the barrier height and the flattening of the barrier in TGSe as compared to that in TGS, the two minima for TGSe are also broader than those of TGS.

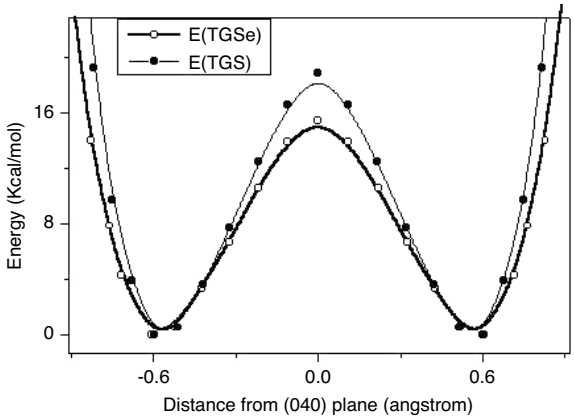

Figure 2. Comparison between the potential seen by the $-NH_3^+$ group in TGS and TGSe.

4. Differences in the ferroelectric phase transition in TGS/TGSe systems

In a large number of crystals the structural phase transitions involve restructuring of only a small fraction of the total structure with the overall structure remaining intact. For example, the structural phase transition in the TGS family primarily involves the dynamic flipping of the amino group ($-NH_3^+$) of GI about the *b*-plane [10]. Flip-flop motion of the hydrogen atom between GII and GIII is a consequence of the amino group motion [10], and hence it plays only a secondary role in the ferroelectric phase transition in the TGS family. A very simplified theory can be constructed from an effective Hamiltonian which takes into account only the motion of these particular coordinates, which broadly characterized the phase transition, treating rest of the crystal lattice as a bath [2]. Hence the dynamics of the ionic system in the TGS/Se system will now be described in the local mode approximation in terms of the local coordinates ($\mathbf{r}$, $\mathbf{p}$) describing the motion of the amino group of GI about the *b*-plane alone. Under static mean field approximation [34] all cells, except the one of immediate interest, are replaced by their thermally averaged configuration and hence the single cell local Hamiltonian H_L becomes

$$H_L(\mathbf{r}) = [H_{\text{single cell}}(\mathbf{r})] + [H_{\text{intercell}}(\mathbf{r})] = [\mathbf{p}^2/2m + Vs(\mathbf{r})] + [-J\langle\mathbf{r}\rangle\mathbf{r}/2].$$

We can in principal separate out the dielectric response of the TGS family into the local and cooperative contributions. The nature, origin and magnitude of the long-range cooperative dipolar interactions in TGS and TGSe are almost identical [35] ($E_{\text{dipolar}}(\text{TGSe}) = 0.62$ kcal mol^{-1} and $E_{\text{dipolar}}(\text{TGS}) =$

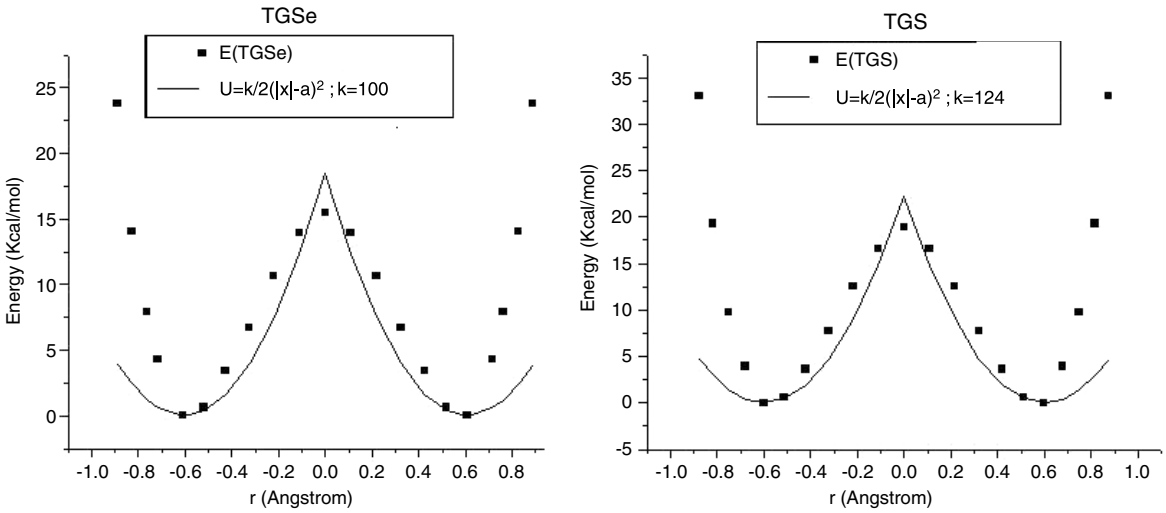

Figure 3. Fit of the net hydrogen-bond energy of the $-NH_3^+$ group to the potential function $U = k^2\{|r| - a\}^2/2$, where r is the distance of nitrogen atom of $-NH_3^+$ group from the b-plane.

0.66 kcal mol^{-1}). These long-range dipolar interactions arise due to the reorientable dipole moments ($\boldsymbol{\mu} = \boldsymbol{\mu}(-NH_3^+) \approx$ 1.4 D) associated with the non-planar amino group of GI. Hence the differences in the phase transition properties of these two might be attributed mainly to the difference in their local motion.

The most commonly accepted model for order–disorder ferroelectrics is 'the Ising model in a transverse field' proposed by Gonzalo *et al* [36, 37]. Within the framework of this model the cooperative contribution is taken care of by the dipole–dipole interaction term J and the local contribution is taken care of by the zero point energy ($h\omega$) term, which is nothing but the measure of the tunneling frequency in a double well local potential. This Ising model in a transverse field has been used for a long time to describe ferroelectric phase transitions. Quantum tunneling and zero point energy effects in double potential wells have been shown [38–40] to give rise to an anomalous behavior at the phase transitions. Through Monte Carlo simulations Gonzalo *et al* [36] showed that the increase in zero point energy not only results in a decrease in the Tc but also the change in the nature of the phase transition. It was shown that only when the zero point energy is very small is the phase transition of the classical second order type.

Since at the microscopic level the main difference between TGS and TGSe is in the double well local potential, this leads us to the conclusion that the most likely source of the difference in the phase transition in these two is the effect of zero point energy. It is observed that as we go from TGS to TGSe there is a decrease in the barrier height of the local single cell potential Vs and the peak of the barrier is flattened. The amino group of GI in TGSe encounters a shallower potential and hence will have a larger zero point energy as compared to that in TGS. In order to get an estimate of the difference in the zero point energy of TGS and TGSe, we have described their respective local single cell potential by a double harmonic form:

$$Vs(r) \sim U(r) = k^2\{|r| - a\}^2/2.$$

The value of the potential parameter k for TGS and TGSe was found to be 124 Å^{-2} kcal mol^{-1} and 100 Å^{-2} kcal mol^{-1}, respectively. This potential function describes the potential barrier at the b-plane ($r \sim 0$) well though the discrepancy between this potential function and the calculated energy increases for larger values of r (figure 3). Since we are interested in the motion of the amino group across the potential barrier at the b-plane we expect this potential to give a good estimate of the tunneling frequency. The tunneling frequency (Ω) for this double harmonic potential is given by the following expression:

$$\Omega = 2\omega_0\sqrt{[2V_0/\pi\hbar\omega_0]}\exp[-2V_0/\hbar\omega_0],$$

where $\hbar\omega_0 = \hbar\sqrt{(k/M)}$ is the ground state energy of the particle in this potential and V_0 is the maximum barrier height at $r = 0$. Using this expression the tunneling frequencies for TGS and TGSe were found to be of the order of 4.6×10^{-9} s^{-1} and 2.0×10^{-7} s^{-1}, respectively. Hence we conclude that the tunneling frequency, which is also the measure of the zero point energy, is an order of magnitude higher for TGSe as compared to that for TGS. We suggest that this difference in the zero point energy of TGS and TGSe, resulting from the difference in the shape of their local potential, might be responsible for the change in the nature of the ferroelectric phase transition in this family.

5. Effect of alanine doping on the phase transition in TGS/TGSe system

In order to investigate the effect of alanine substitution on the phase transition properties of the TGS/TGSe system, crystals of L-alanine doped TGS and TGSe ($(glycine)_{3x}(alanine)_{3(1-x)}H_2AO_4$, where A = S or Se and x = 1.0, 0.9 and 0.8) were grown by the solution method. Since the alanine molecule [$CH_3CHCOOHNH_2$] is similar to the glycine [$CH_2COOHNH_2$] molecule it is expected to substitute glycine in some unit cells. DSC measurements were

Table 4. Variation in the hydrogen-bond energies, calculated using the Lippincott and Schroeder function, for the hydrogen bonds made by the $-NH_3^+$ group of GI as it moves away from the *b*-plane. Dis gives the distance of the $-NH_3^+$ group from the *b*-plane; the net potential energy of the group is taken as the sum of the hydrogen-bond energies.

	TGSe				TGS			
N–H–O	H–O Å (*d*)	N–O Å (*R*)	Ene. (kcal mol^{-1})	Dis. (Å)	H–O Å (*d*)	N–O Å (*R*)	Ene. (kcal mol^{-1})	Dis. (Å)
N1e–H1–O12	2.371	2.641	16.563		2.317	2.627	18.855	
N1e–H2–O2se/O2s	2.096	2.926	−2.081		2.026	2.928	−2.759	
N1e–H2–O3se/O3s	2.096	2.926	−2.081		1.996	2.862	−1.943	
N1e–H3–O22	2.401	3.303	−1.595		2.386	3.272	−1.669	
			10.806	0.00			12.484	0.000
N1d–H1–O12	2.264	2.647	15.323		2.211	2.634	17.241	
N1d–H2–O2se/O2s	2.029	2.878	−1.914		1.968	2.884	−2.794	
N1d–H2–O3se/O3s	2.169	2.978	−2.103		2.057	2.909	−2.181	
N1d–H3–O22	2.277	3.208	−2.024		2.259	3.178	−2.112	
			9.282	0.110			10.154	0.110
N1c–H1–O12	2.177	2.666	12.221		2.124	2.653	13.718	
N1c–H2–O2se/O2s	1.967	2.837	−1.659		1.918	2.847	−2.733	
N1c–H2–O3se/O3s	2.245	3.035	−2.042		2.123	2.960	−2.245	
N1c–H3–O22	2.164	3.116	−2.558		2.141	3.086	−2.672	
			5.962	0.219			6.068	0.217
N1b–H1–O12	2.112	2.695	8.402		2.058	2.682	9.381	
N1b–H2–O2se/O2s	1.913	2.803	1.332		1.874	2.816	−2.612	
N1b–H2–O3se/O3s	2.323	3.095	1.919		2.191	3.014	−2.196	
N1b–H3–O22	2.064	3.027	3.122		2.036	2.997	−3.255	
			2.029	0.324			1.318	0.321
N1a–H1–O12	2.077	2.734	4.668		2.016	2.720	5.172	
N1a–H2–O2se/O2s	1.876	2.776	0.814		1.839	2.792	−2.450	
N1a–H2–O3se/O3s	2.406	3.156	1.758		2.261	3.017	−1.915	
N1a–H3–O22	1.989	2.943	3.373		1.944	2.913	−3.645	
			−1.277	0.425			−2.838	0.420
N1–H1–O12	2.053	2.780	1.608		1.997	2.765	1.797	
N1–H2–O2se/O2s	1.829	2.755	0.730		1.811	2.776	−2.418	
N1–H2–O3se/O3s	2.481	3.217	1.603		2.331	3.128	−1.916	
N1–H3–O22	1.911	2.866	3.339		1.869	2.835	−3.359	
			−4.064	0.519			−5.896	0.512
N1a′–H1–O12	2.055	2.832	0.466		1.999	2.720	−0.497	
N1a′–H2–O2se/O2s	1.800	2.742	0.677		1.790	2.765	−2.436	
N1a′–H2–O3se/O3s	2.558	3.277	1.450		2.400	3.184	−1.750	
N1a′–H3–O22	1.860	2.795	2.080		1.809	2.763	−1.758	
			−4.673	0.607			−6.449	0.598
N1b′–H1–O12	2.086	2.908	1.909		2.019	2.869	−1.831	
N1b′–H2–O2se/O2s	1.772	2.733	0.899		1.777	2.761	−2.613	
N1b′–H3–O22	1.815	2.709	2.412		1.765	2.698	1.938	
			−0.396	0.715			−2.506	0.678
N1c′–H1–O12	2.116	2.943	2.129		2.052	2.924	−2.440	
N1c′–H2–O2se/O2s	1.773	2.731	0.714		1.769	2.761	−2.877	
N1c′–H3–O22	1.811	2.674	6.061		1.735	2.639	8.582	
			3.218	0.761			3.265	0.750
N1d′–H1–O12	2.152	3.001	2.345		2.909	2.979	−2.603	
N1d′–H2–O2se/O2s	1.752	2.733	1.588		1.767	2.765	−3.177	
N1d′–H3–O22	1.795	2.624	13.270		1.718	2.587	18.646	
			9.337	0.828			12.866	0.816
N1e′–H1–O12	2.202	3.057	2.287		2.146	3.034	−2.525	
N1e′–H2–O2se/O2s	1.755	2.738	1.850		1.770	2.772	−3.466	
N1e′–H3–O22	1.797	2.580	23.250		1.712	2.541	32.530	
			19.113	0.888			26.539	0.875

performed on these doped crystals in the temperature range 253–333 K with the heating rate 5 K min^{-1} (figure 4). DSC results show that the increase in the transition temperature due to alanine doping is about 1 K and there is a significant change in the peak shape, especially for TGSe.

It is observed that the influence of alanine substitution on the ferroelectric phase transition is much more pronounced in TGSe as compared to in TGS. In fact DSC data indicates that the phase transition in L-alanine doped TGSe for large dopant concentrations $(1 - x)$ reflects supercritical behavior [41] i.e. the phase transition is no longer well defined and abrupt but instead gradually changes from paraelectric to ferroelectric behavior. There is no change in the average symmetry of these crystals at the transition, since the symmetry of the

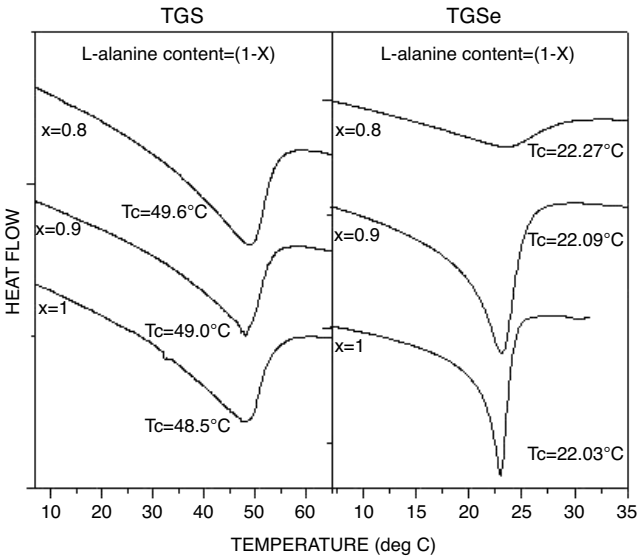

Figure 4. DSC thermograms for L-alanine doped TGS and TGSe crystals with the heating rate of 5 K min^{-1}.

high temperature phase cannot be ideally $P2_1/m$, as there are handed molecules (L-alanine) present at certain sites within these crystals.

In order to estimate the extent of alanine incorporated within these crystals, x-ray powder diffraction patterns of them were recorded and cell parameter refinement was done using Le-bail method as implemented in the software WINMPROF [42]. Since the alanine molecule (molecular volume 97.7 $Å^3$) is bigger in size as compared to the glycine molecule (molecular volume 74.6 $Å^3$), the unit cells in which glycine is substituted by alanine are expected to expand in size in order to incorporate a bigger molecule. Hence the average unit cell volume in the doped crystals is expected to increase. The average unit cell volume of L-alanine doped TGSe with $(1 - x) = 0.2$ was found to be 670.6(4) $Å^3$ (3.8 $Å^3$ greater than pure TGSe) and that of L-alanine doped TGS with $(1 - x) = 0.2$ was found to be 641.0(2) $Å^3$ (0.9 $Å^3$ greater than pure TGS). This indicates that the extent of alanine substitution within the crystal lattice of TGSe is much greater. In order to find the reason for this difference between the amount of alanine molecules incorporated within TGS and TGSe we calculated the crystal packing coefficients for the two crystals. The crystal packing coefficient is defined as the ratio of the molecular volume to the unit cell volume; the values obtained for TGS and TGSe are 0.89 and 0.86, respectively (all molecular volumes are obtained using the program MOLDRAW [43]). This indicates that TGSe unit cell has bigger voids as compared to that of TGS. Hence TGSe crystals can accommodate a greater number of dopant molecules. This fact is supported by the higher value for the volume compressibility of TGSe (5.3×10^{-11} m^2 N^{-1}) as compared to that of TGS (4.4×10^{-11} m^2 N^{-1}) (the TGS and TGSe volume compressibility is calculated using their respective elastic stiffness coefficients [44, 45]). Since the number of alanine molecules substituting the glycine molecule is much greater in TGSe the effect of doping on the phase transition is much more pronounced in TGSe.

6. Conclusions

The crystal structures of TGS and TGSe obtained from single crystal neutron diffraction were compared and it was found that the shape of the unit cell as well as the atomic coordinates in these two crystals are very similar, the difference being mainly in the cell volume, which is higher in the case of TGSe. The double well local potential (Vs) seen by the amino group of GI in TGS and TGSe was obtained using their crystal structure. It is suggested that the change in the nature of the ferroelectric phase transition as one goes from TGS to TGSe is due to the increase in the zero point energy resulting due to the change in the shape and height of the double well local potential of these crystals.

It is observed that the influence of alanine substitution on the ferroelectric phase transition is more pronounced in TGSe as compared to that in TGS. This difference is mainly due to the fact that TGSe crystals can accommodate many more dopant molecules than TGS crystals. The high level of alanine doping in these crystals makes their phase transition supercritical i.e. the phase transition is no longer well defined and abrupt but instead gradually changes from paraelectric to ferroelectric behavior. There is no change in the average symmetry of these doped crystals across the phase transition temperature.

Acknowledgment

The authors thank Dr Lata Panicker, of SSPD BARC, for carrying out DSC measurements.

References

[1] Wadhawan V K 2000 *Introduction to Ferroic Materials* (London: Gordon and Breach)
[2] Lines M E and Glass A M 1977 *Principles and Applications of Ferroelectrics and Related Materials* (Oxford: Clarendon)
[3] Hayward S A and Salje E K H 1998 *J. Phys.: Condens. Matter* **10** 1421
[4] Onodera Y 1970 *Prog. Theor. Phys.* **44** 1477
[5] Onodera Y 1971 *Prog. Theor. Phys.* **45** 986
[6] Onodera Y and Kojyo N 1989 *J. Phys. Soc. Japan* **58** 3227
[7] Onodera Y and Sawahima N 1991 *J. Phys. Soc. Japan* **60** 1247
[8] Gadekar S N and Ramakrishnan T V 1980 *J. Phys. C: Solid State Phys.* **13** L957
[9] Imry Y 1974 *Phys. Rev. Lett.* **33** 1304
[10] Choudhury R R, Chitra R and Ramanadham M 2003 *J. Phys.: Condens. Matter* **15** 4641
[11] Choudhury R R, Chitra R and Ramanadham M 2004 *Phase Transit.* **77** 385
[12] Matthias B T, Miller C E and Remeika J P 1956 *Phys. Rev.* **104** 849
[13] Jona F and Shirane G 1962 *Ferroelectric Crystals* (Oxford: Pergamon) chapter 2
[14] Gonzalo J A and Lopez-Alonso J R 1964 *J. Phys. Chem. Solids* **25** 303
[15] Gonzalo J A 1970 *Phys. Rev.* B **1** 3125
[16] Gonzalo J A 1974 *Phys. Rev.* B **9** 3149

[17] Stankowski J 1981 *Phys. Rep.* **77** 1
[18] Fugiel B and Mierzwa M 1998 *Phys. Rev.* B **57** 777
[19] Koralewski M, Stankowska J, Iglesias T R and Gonzalo J A 1996 *J. Phys.: Condens. Matter* **8** 4079
[20] Castillo J R F D, Gonzalo J A and Przeslawski J 2000 *Physica* B **292** 23
[21] Romero F J, Gallardo M C, Jimenez J, Czarnecka A, Koralewski M and Cerro J D 2004 *J. Phys.: Condens. Matter* **16** 7637
[22] Tylczynski Z, Karaev A D and Mroz B 2000 *J. Phys.: Condens. Matter* **12** 7133
[23] Choudhury R R, Chitra R, Ramanadham M and Javeyl R 2002 *Appl. Phys.* A **74** S1667
[24] Choudhury R R, Poswal H K, Chitra R and Sharma S M 2007 *J. Chem. Phys.* **127** 154712
[25] Choudhury R R and Chitra R 2008 *Pramana J. Phys.* **71** 911
[26] Sheldrick G M 1997 *SHELXL97* University of Gottingen, Germany
[27] Fabian L and Kalman A 1999 *Acta Crystallogr.* B **55** 1099
[28] Horiuchi S and Kumai R 1998 *J. Am. Chem. Soc.* **120** 7379
[29] Horiuchi S, Kumai R and Okimoto Y 1999 *Phys. Rev.* B **59** 11267
[30] Kikuta T, Hamatake D, Yamazaki T and Nakatani N 2007 *Ferroelectrics* **347** 65
[31] Lippincott E R and Schroeder R 1957 *J. Phys. Chem.* **61** 921
[32] Chidambaram R and Sikka S K 1968 *J. Chem. Phys. Lett.* **2** 162
[33] Ramanadham M and Chidambaram R 1978 *Advances in Crystallography* ed R Srinivasan (New Delhi: Oxford–IBH Press) p 81
[34] Lines M E 1977 *Phys. Rev.* B **15** 388
[35] Choudhury R R, Chitra R and Ramanadham M 2005 *Physica* B **366** 116
[36] Wang C L, Garcia J, Arago C, Gonzalo J A and Marques M I 2002 *Physica* A **312** 181
[37] Wang C L, Arago C, Garcia J and Gonzalo J A 2002 *Physica* A **308** 337
[38] Gonzalo J A 1989 *Phys. Rev.* B **39** 12297
[39] Gonzalo J A 1995 *Ferroelectrics* **168** 1
[40] Aragó C and Gonzalo J A 2000 *J. Phys.: Condens. Matter* **12** 3737
[41] Kumar S 2001 *Liquid Crystal: Experimental Studies of Physical Properties and Phase Transitions* (Cambridge: Cambridge University Press) chapter 7
[42] Jouanneaux A 1999 *CPD Newslett.* **21** 13
[43] Ugliengo P, Barzani G and Viterbo D 1993 *Z. Kristallogr.* **9** 207
[44] Hatano J, Suda F and Futama H 1977 *J. Phys. Soc. Japan* A **43** 1933
[45] Dunk A and Saunders G A 1984 *J. Mater. Sci.* **19** 125